Journal of Digital Ecosystem for Natural Sustainability (JoDENS)
Vol.6, No.1, Juli 2026, pp. 68~74
e-ISSN: 2798-6179
DOI: https://doi.org/10.63643/jodens.v6i1.386

ArachnoSAR: A Quadruped Spider Robot Prototype with Haar Cascade-Based Face Detection to Support Search and Rescue Operations

James Lim [1], Eril Sanjaya [2], Fernando [3*], Augustian Gautama [4], Tino Winata Sumarno [5], Canniago Verrian [6], Andi Saputra [7], Agus Suwandi [8], Raymond Erz Saragih [9]
[1]*Informatics Engineering Study Program, Universitas Universal, Batam, Indonesia*
**Corresponding author E-mail: fernando.lee633@uvers.ac.id*

Article Info

Article history:

Received 10-07-2026
Revised 20-07-2026
Accepted 28-07-2026

Keyword:

Face detection, Haar Cascade, image processing, quadruped robot, search and rescue

ABSTRACT

Search and rescue (SAR) operations often require access to areas that are hazardous or unreachable for human rescuers. This study developed ArachnoSAR, a low-cost four-legged (quadruped) spider robot prototype that integrates legged locomotion, camera-based human detection, and automatic notification. The robot is driven by eight SG90 servo motors controlled by an ESP32, while a Raspberry Pi processes the camera stream using a Haar Cascade classifier and sends detection photographs to a Telegram bot, accompanied by a buzzer alert. Preliminary indoor testing showed that the system detected frontal faces at distances of up to 300 cm at 12 to 17 frames per second, while locomotion tests recorded speeds of 0.55 cm/s on ceramic and 1.36 cm/s on asphalt surfaces, with an estimated operating time of about 51 minutes. Identified limitations include the requirement for frontal face orientation, sensitivity to low lighting, motion blur, and dependence on internet connectivity for notification. These results indicate that the prototype is feasible as a proof of concept, while highlighting the need for image stabilization, deep learning based detection, and offline communication for real SAR deployment.

I. INTRODUCTION

Search and rescue (SAR) operations frequently require the exploration of areas that are hazardous or difficult to reach, such as collapsed buildings, unstable terrain, and densely vegetated regions. Manual monitoring poses a high risk to the safety of rescue teams and must be performed within a limited time window, so robotic systems capable of assisting in detecting human presence have the potential to reduce these risks while accelerating the rescue process [1]. A comprehensive review of rescue robotics also indicates that a considerable gap remains between research capabilities and the actual needs of first responders, making the development and evaluation of prototypes a continuing necessity [2].

Legged robots are among the most widely developed architectures for uneven terrain because their legs can adapt to surfaces that wheeled vehicles cannot traverse [3], [4]. At the state-of-the-art level, the ANYmal quadruped robot combined with aerial robots has demonstrated autonomous exploration of underground environments and won the DARPA Subterranean Challenge [5]; however, such platforms demand very high cost and complexity. On the other hand, low-cost quadruped spider robots have been developed for exploration and data gathering in areas dangerous to humans [6], [7]. The quadruped design was chosen in this study because it offers a balance between stability, mechanical simplicity, and a smaller number of actuators compared to six- or eight-legged designs.

Another challenge in SAR missions is the victim detection process itself. Victims generally occupy only a small fraction of pixels in an image, may be covered by vegetation or debris, and may lie in unusual body positions, so prolonged manual observation of video feeds is highly fatiguing for operators [8]. Automatic human detection capability on the robot therefore becomes an essential requirement.

For image-based human detection, deep learning approaches such as convolutional neural networks (CNN) have been proven to provide high accuracy and robustness [8], [9], including lightweight YOLO variants designed for deployment on resource-constrained devices [10]. Nevertheless, on very low-cost prototypes with computing power comparable to a Raspberry Pi, classical methods such as the Haar Cascade Classifier [11] remain relevant as a baseline due to their small computational requirements. Prior work by the present research group has applied this low-cost, vision-based approach to an automated guided vehicle for image-processing-based package sorting (CAGO) [12] and to a 4-DOF camera arm employing a cascade classifier for human detection and a PCA9685 servo driver (Glambot SNAFH-R1) [13]; however, an affordable prototype that integrates quadruped locomotion, on-board human detection, and real-time notification within a single complete system remains rarely documented, particularly in the context of development in Indonesia.

Based on these considerations, this study developed ArachnoSAR, a quadruped spider robot prototype to support SAR missions. The contributions of this study include: (1) the design and construction of a four-legged quadruped prototype with eight servo motors based on a PCA9685 driver and a dual ESP32–Raspberry Pi controller; (2) the end-to-end integration of Haar Cascade-based face detection with automatic notification via Telegram and a buzzer; and (3) a preliminary evaluation covering detection distance, parameter effects, processing speed, locomotion speed on two surface types, and power consumption. All tests were conducted under controlled indoor conditions, so the results of this study are positioned as a proof of concept rather than a validation under actual disaster conditions.

II. METHOD

A. System Architecture

The ArachnoSAR system uses two controllers working in tandem. The ESP32 controls eight servo motors through a PCA9685 PWM driver module (16 channels, 12-bit resolution) commanded via the I2C interface, while the Raspberry Pi handles image acquisition and processing from the webcam as well as notification delivery. The two controllers communicate through a serial interface.

The system workflow begins when the switch is turned on: both controllers initialize the actuators and camera, the robot enters standby mode, and then moves forward while scanning the camera feed. When a human is detected within the field of view, the Raspberry Pi sends the detection photograph to a Telegram bot and activates a buzzer as an audible marker at the location. Figure 1 shows the system integration diagram, while the complete workflow is shown in Figure 2.

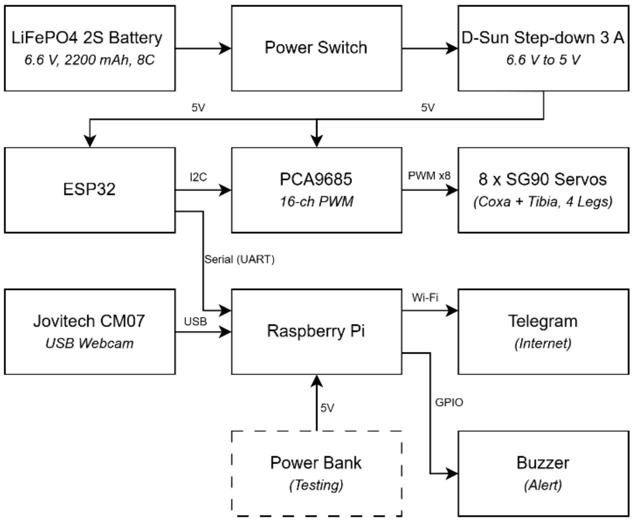

Figure 1. ArachnoSAR system integration diagram

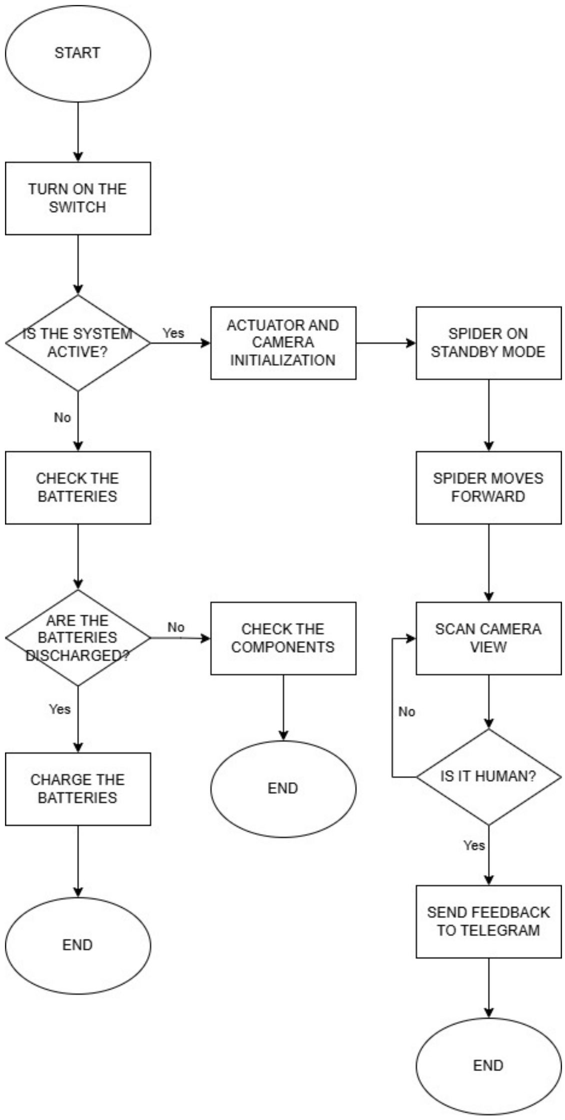

Figure 2. Prototype workflow flowchart

B. Hardware

The main components of the prototype are summarized in Table 1. The main frame was 3D-printed from PETG filament using the fused deposition modeling (FDM) method. PETG was selected for its balance of mechanical strength, flexibility, moisture resistance, and light weight; the mechanical characterization of FDM-printed PETG reported in the literature indicates adequate tensile strength accompanied by a tendency toward brittleness under certain conditions [14]. The SG90 servo motor was selected for its small size, light weight, affordability, and ease of control through PWM signals.

Table 1. Main components of the ArachnoSAR prototype

Component	Qty	Function
PETG frame (3D-printed)	1 set	Main robot structure
SG90 Tower Pro servo	8	2-DOF actuation per leg
Jovitech CM07 webcam	1	1080p image acquisition
Raspberry Pi	1	Image processing and notification
ESP32	1	Motion control and serial communication
PCA9685 servo driver	1	16-channel 12-bit PWM generator (I2C)
D-Sun 3 A DC-DC step-down	1	6.6 V → 5 V regulation
LiFePO4 2S 6.6 V 2200 mAh battery	1	Main power source (8C rating)
Buzzer	1	Audible alert upon detection
Switch, PCB, pin headers, terminals	—	Integration and power distribution

The main power source is a two-cell lithium iron phosphate (LiFePO4) battery with a nominal voltage of 6.6 V, a capacity of 2200 mAh, and an 8C discharge rating, giving a maximum continuous current of 17.6 A — well above the system load requirement. A D-Sun DC-DC step-down module rated at 3 A converts the battery voltage to a single 5 V rail that supplies the servo power rail at the PCA9685 V+ terminal as well as the system logic. The power requirements of each component are summarized in Table 2.

Table 2. Component power requirements

Component	Qty	Voltage	Current	Power	Total
Raspberry Pi	1	5 V	2.5 A	12.5 W	12.5 W
ESP32	1	3.3 V	0.16 A	0.528 W	0.528 W
SG90 servo	8	5 V	0.25–0.8 A	1.25–4 W	10–32 W
Jovitech CM07 webcam	1	5 V	0.15 A	1 W	1 W

The servo current range in Table 2 spans the measured operating current under moderate load (approximately 0.25 A per servo; Section III.D) up to the maximum stall current according to the vendor datasheet (0.8 A); the power design refers to the upper bound as the worst-case condition.

C. Software

The ESP32 firmware was developed using the Arduino IDE to read serial commands and drive the PCA9685 servo driver through the I2C interface. Image processing on the Raspberry Pi was implemented with Python 3.10 and the OpenCV library. Notification utilizes the Telegram bot API, following common practice in IoT-based monitoring systems [15]. System diagrams were designed using draw.io and the electronic schematic using EasyEDA.

D. Mechanical Design and Gait Pattern

Each leg consists of two segments, the coxa (connecting the leg to the body) and the tibia (the main actuation segment), each driven by one servo motor, giving a total of eight servos for four legs (2 DOF per leg). This configuration imitates the basic structure of spider legs, with the number of legs simplified to four.

The reference angles of each servo in the default and standing positions are summarized in Table 3. The forward gait pattern is implemented as a sequence of angle commands with a delay of 100 ms per step (50 ms at initialization), as summarized in Table 4.

Table 3. Servo reference angles

Position	Right Front	Left Front	Back Right	Back Left
Default — Coxa	90°	90°	90°	90°
Default — Tibia	90°	90°	90°	90°
Standing — Coxa	120°	120°	120°	120°
Standing — Tibia	160°	160°	160°	160°

Table 4. Forward gait sequence (angle commands per step)

FLT	FLC	BLT	BLC	FRT	FRC	BRT	BRC	MS
dpt	dpc	dpt	dpc	dpt	dpc	dpt	dpc	50
115°	160°	dpt	dpc	dpt	dpc	dpt	dpc	100
dpt	160°	dpt	dpc	dpt	dpc	dpt	dpc	100
dpt	160°	dpt	dpc	dpt	dpc	120°	90°	100
dpt	160°	dpt	dpc	dpt	dpc	dpt	90°	100
dpt	dpc	dpt	dpc	dpt	dpc	dpt	dpc	100
dpt	dpc	dpt	dpc	90°	160°	dpt	dpc	100
dpt	dpc	dpt	dpc	dpt	160°	dpt	dpc	100
dpt	dpc	100°	90°	dpt	160°	dpt	dpc	100
dpt	dpc	170°	90°	dpt	160°	dpt	dpc	100
dpt	dpc	dpt	dpc	dpt	dpc	dpt	dpc	100

Notes for Table 4: F = front, B = back, L = left, R = right, T = tibia, C = coxa; MS = inter-command delay (milliseconds); dpt = default tibia angle (160°); dpc = default coxa angle (120°). The first row is the initialization step (50 ms); each subsequent gait step is executed with a 100 ms delay.

E. Face Detection and Notification

Human detection is implemented as face detection using the Haar Cascade Classifier introduced by Viola and Jones [11], with a pre-trained model from OpenCV. The method exploits Haar-like features that measure the contrast between dark and light regions of an image, with staged (cascade) classification trained using AdaBoost, making it lightweight enough to run on devices with limited computing power and widely used for face detection [16], [17]. The processing flow is shown in Figure 3: the input image is converted to grayscale and processed by the detectMultiScale function; if a face is detected, the photograph is sent to Telegram and the buzzer is activated.

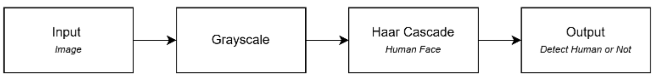

Figure 3. Image processing flow for face detection

Three detectMultiScale parameter configurations were tested: (1.1, 7), (1.1, 9), and (1.2, 7), all with a minSize of (50, 50). The configuration (1.2, 7) was selected as the final configuration. The meaning of each parameter is summarized in Table 5.

Table 5. detectMultiScale parameters used

Parameter	Final value	Description
scaleFactor	1.2	Image downscaling factor per scale; smaller values are more thorough but slower
minNeighbors	7	Higher values are stricter (fewer false positives, but small faces may be missed)
minSize	(50, 50)	Faces smaller than this size are ignored

F. Testing Procedure

Five tests were conducted under controlled indoor conditions: (1) observation of the rigidity and durability of the PETG frame during assembly and operation; (2) servo response and gait pattern testing; (3) face detection testing with parameter and distance variations, with detection results sent to Telegram; (4) current consumption measurement using a multimeter, with the Raspberry Pi powered separately through a power bank; and (5) locomotion testing over a distance of 60 cm on ceramic and asphalt surfaces with travel time recording.

III. RESULTS AND DISCUSSION

A. PETG Frame Performance

The frame was printed with the parameters listed in Table 6, and the fully assembled prototype is shown in Figure 4. During assembly and operation, the PETG structure exhibited good rigidity and dimensional stability in supporting the eight servos and the electronic components, and was able to dampen moderate vibrations. Minor surface deformation was observed without affecting function. The identified weakness is a tendency toward brittleness at points subjected to repeated stress, such as bolt holes and small mechanical joints; this finding is consistent with the brittle characteristics of FDM-printed PETG reported in the literature [14], so design tolerances at these points require attention.

Table 6. Frame printing parameters

Material	Fill density	Extruder temp.	Platform temp.
Flash-Forge PETG	100%	240 °C	80 °C

Figure 4. The assembled ArachnoSAR prototype: four 2-DOF legs driven by eight SG90 servos, a front-mounted Jovitech CM07 webcam, and on-board control electronics

B. Servo Response and Locomotion

Servo actuation through PWM signals from the PCA9685 controlled by the ESP32 produced accurate angular responses with minimal delay, and the damping characteristics of the PETG frame helped maintain stability during step transitions. The average locomotion speed is calculated using Equation (1):

$$v = \frac{s}{t} \tag{1}$$

where v is the speed (cm/s), s is the distance traveled (cm), and t is the travel time (s). The locomotion test results on the two surfaces are summarized in Table 7.

Table 7. Locomotion test results (60 cm travel distance)

Surface	Travel time	Speed
Ceramic	1 min 50 s	0.55 cm/s
Asphalt	44 s	1.36 cm/s

The robot moved more slowly on ceramic because the slippery surface caused the legs to lose traction and slip, whereas the rough texture of asphalt improved grip, resulting in more stable and faster movement. This finding shows that surface type significantly affects the movement efficiency of wheel-less legged robots, and should be considered in selecting foot materials in future development.

C. Face Detection and Notification

With the final configuration (1.2, 7, (50, 50)), the system consistently detected frontal faces up to a maximum distance of 300 cm, with the subject's face positioned at a height of 80–90 cm above the floor, as the subject was seated on the floor during testing. The processing speed recorded on the screen captures ranged from 12.29 to 17.15 frames per second. An example of a detection result sent to Telegram is shown in Figure 5. The buzzer activated on every detection, assisting the on-site localization of the robot and the victim.

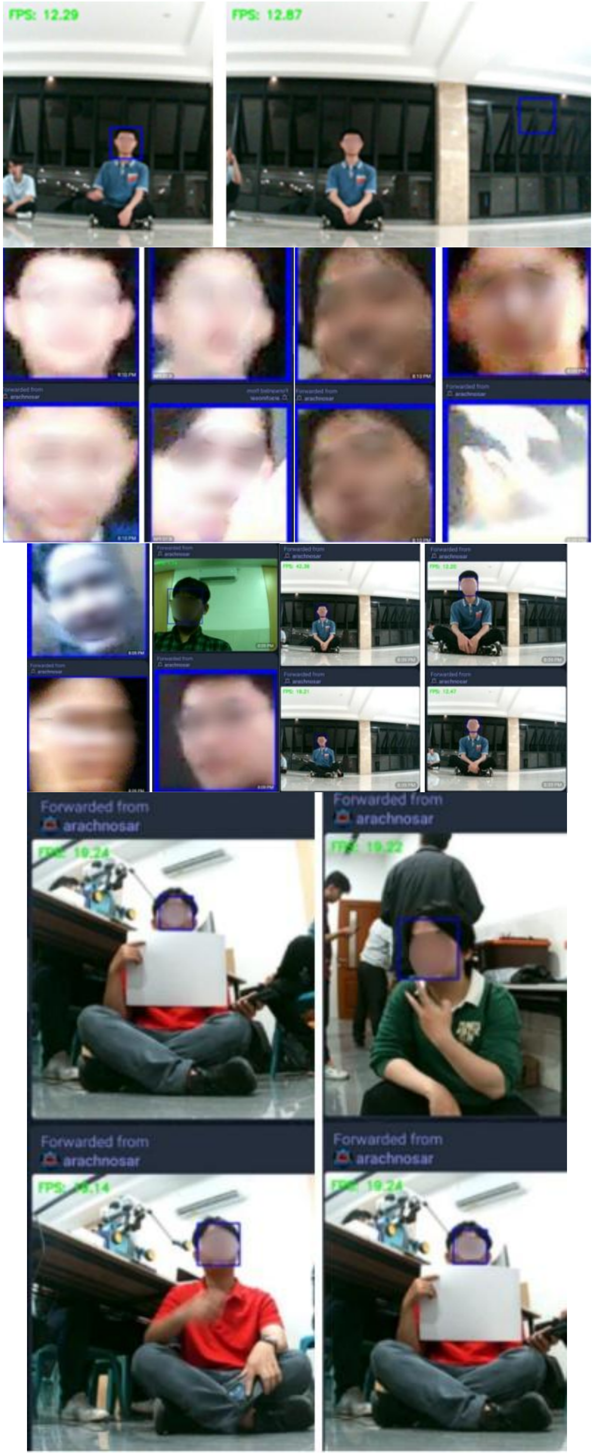

Figure 5. Example of a detection result sent to Telegram

Three constraints were identified during testing. First, images became blurred while the robot was moving, especially on uneven surfaces, because stepping vibrations were transmitted to the camera mount, which has no stabilization. Second, under low lighting, the automatic white balance failed to adjust colors, making subjects appear pale and reducing detection performance. Third, detection requires the face to be frontal to the camera; tilted, sideways, or partially covered faces generally failed to be detected.

D. Power Consumption

Multimeter measurements showed an operating current of approximately 250 mA per servo under moderate load, reaching approximately 600 mA when approaching stall, or a total of 2.0–4.8 A for the eight servos. The operating duration is estimated using Equation (2):

$$t_{op} = \frac{E_b \eta}{P_L} \tag{2}$$

where t^{op} is the operating duration (h), E^{b} is the battery energy (Wh), η is the step-down conversion efficiency, and P^{L} is the total load power (W). The battery energy is the product of the nominal voltage and the capacity, i.e., 6.6 V × 2.2 Ah = 14.52 Wh. Assuming η = 0.87 (the typical 85–90% range for buck modules) and a 5 V servo rail from the D-Sun module, the measured load of 10.5–24.5 W yields an estimate of 31–72 minutes, with an average of about 51 minutes. This estimate excludes the Raspberry Pi, which was powered separately through a power bank during testing; if the Raspberry Pi (rated at 12.5 W) and the webcam were powered from the main battery, the projected duration drops to approximately 20–32 minutes. Notably, the system bottleneck is not the battery — the 8C rating corresponds to a continuous current of 17.6 A — but the step-down module: the measured peak servo load (±4.8 A near stall; theoretically up to 6.4 A if all eight servos stall according to the datasheet) exceeds the module's 3 A rating, so a higher-capacity regulator is recommended for the next iteration.

With a speed of 0.55–1.36 cm/s and an average duration of about 51 minutes, the effective travel range per charge is in the range of 17–42 meters, assuming continuous movement. This figure emphasizes that power management and locomotion efficiency are critical aspects that must be improved before the prototype can be considered for actual SAR missions.

E. Discussion, Limitations, and Future Development

Overall, the test results show that the integration of quadruped locomotion, on-board face detection, and automatic notification in a single low-cost prototype can function end-to-end. The position of this study relative to related work is summarized in Table 8.

Table 8. Comparison with related work

Study	Platform	Victim/object detection	Remarks
Tranzatto et al. [5]	ANYmal (quadruped) + aerial robots	Multi-modal perception, autonomous object detection	DARPA SubT winner; very high cost and complexity
Cruz Ulloa et al. [18]	Quadruped + thermal and RGB cameras	CNN on thermal imagery	Validated in rescue simulations; effective in low light
Kannan et al. [6]	Low-cost quadruped spider, 3 DOF per leg	—	Focus on locomotion and data gathering (ESP32-CAM visual feed)
Gaur et al. [7]	Low-cost quadruped spider	—	Focus on mechanical design and control

Sambolek & Ivasic-Kos [8]	Aerial imagery (not a ground robot)	Deep CNN detectors	Focus on evaluating human detection algorithms for SAR
ArachnoSAR (this study)	8-servo SG90 quadruped, ESP32 + Raspberry Pi	On-board Haar Cascade (face)	Telegram + buzzer notification; low-cost prototype, indoor testing

Compared to research-grade platforms such as ANYmal [5] or autonomous thermal detection systems [18], ArachnoSAR occupies the niche of a very low-cost educational prototype, with consequently far more limited capabilities. The choice of Haar Cascade proved able to run on the Raspberry Pi with adequate processing speed — the observed 12.29–17.15 frames per second compares favorably with the roughly 2 frames per second reported for a YOLOv5s detector on an embedded Jetson Nano platform [10] — but its accuracy and robustness fall below those of deep learning-based detectors reported in the SAR literature [8], [10], and it is highly dependent on object orientation, as is characteristic of Haar feature-based methods [17].

The limitations of this study need to be stated explicitly. First, detection only works on frontal faces, whereas disaster victims typically lie down or are partially covered; deep learning-based body or body-part detection [10], [19] is a more suitable direction for improvement. Second, performance degrades under low lighting and while the robot is moving, due to blur. Third, notification depends on internet connectivity for Telegram, while cellular networks are often disabled in disaster zones; LoRa-based mesh networks proposed for post-disaster emergency communication [20] are a viable alternative to examine. Fourth, the operating duration and travel range remain very limited. Fifth, all testing was conducted indoors; performance on rubble, outdoor terrain, and in adverse weather has not been validated.

From an ethical standpoint, the robot's camera can potentially record personal data such as victims' faces and property at disaster sites. Recording management should follow personal data protection principles as regulated by Law of the Republic of Indonesia Number 27 of 2022 on Personal Data Protection [21], covering access restriction, retention periods, and the purposes of data use.

Future development is directed toward: adding camera stabilization and an IMU sensor to reduce blur and maintain movement stability; replacing the detector with lightweight deep learning models capable of recognizing bodies in various poses [10], [19]; adding a thermal camera, which has proven effective for victim recognition in low-light conditions [18]; semi-autonomous navigation with obstacle avoidance and coordinate marking; sound detection to complement visual detection; and communication channels that do not depend on the internet [20].

IV. Conclusion

This study successfully built ArachnoSAR, a low-cost quadruped spider robot prototype integrating eight-servo locomotion, Haar Cascade-based face detection on a Raspberry Pi, and automatic notification via Telegram and a buzzer. Preliminary indoor testing showed frontal face detection up to a distance of 300 cm at a processing speed of 12–17 frames per second, locomotion speeds of 0.55 cm/s on ceramic and 1.36 cm/s on asphalt surfaces, and an estimated operating duration of about 51 minutes excluding the Raspberry Pi load.

These results demonstrate the feasibility of the integration concept on a low-cost prototype, while also underlining its limitations: the requirement for frontal face orientation, sensitivity to lighting and motion, dependence on the internet, and limited operating duration and range. Improvements in image stabilization, deep learning-based detectors, complementary sensors such as thermal cameras, and offline communication are prerequisites before similar systems can be tested in actual SAR scenarios.

References

[1] K. Sharma, R. Doriya, S. K. Pandey, A. Kumar, G. R. Sinha, and P. Dadheech, "Real-time survivor detection system in SaR missions using robots," Drones, vol. 6, no. 8, p. 219, 2022.

[2] J. Delmerico et al., "The current state and future outlook of rescue robotics," Journal of Field Robotics, vol. 36, no. 7, pp. 1171-1191, 2019.

[3] P. Biswal and P. K. Mohanty, "Development of quadruped walking robots: A review," Ain Shams Engineering Journal, vol. 12, no. 2, pp. 2017-2031, 2021.

[4] C. Cruz Ulloa, L. Sanchez, J. Del Cerro, and A. Barrientos, "Deep learning vision system for quadruped robot gait pattern regulation," Biomimetics, vol. 8, no. 3, p. 289, 2023.

[5] M. Tranzatto et al., "CERBERUS in the DARPA Subterranean Challenge," Science Robotics, vol. 7, no. 66, eabp9742, 2022.

[6] C. S. Kannan, R. P. Rangan, K. Nithish, S. Amanullah, K. Akash, and S. P. H. Prasaath, "Spider bot - a quadruped robot for data gathering," Journal of Engineering Science and Technology Review, vol. 15, no. 6, pp. 15-19, 2022.

[7] D. Gaur, J. Varshney, A. Maryam, and S. Gautam, "QuadraSpider: a four-legged spider robot design and control," International Research Journal of Engineering and Technology, vol. 10, no. 9, 2023.

[8] S. Sambolek and M. Ivasic-Kos, "Automatic person detection in search and rescue operations using deep CNN detectors," IEEE Access, vol. 9, pp. 37905-37922, 2021.

[9] K. H. Teoh, R. C. Ismail, S. Z. M. Naziri, R. Hussin, M. N. M. Isa, and M. S. S. M. Basir, "Face recognition and identification using deep learning approach," Journal of Physics: Conference Series, vol. 1755, p. 012006, 2021.

[10] F. Ciccone and A. Ceruti, "Real-time search and rescue with drones: A deep learning approach for small-object detection based on YOLO," Drones, vol. 9, no. 8, p. 514, 2025.

[11] P. Viola and M. Jones, "Rapid object detection using a boosted cascade of simple features," in Proc. IEEE Conf. on Computer Vision and Pattern Recognition (CVPR), 2001, pp. 511-518.

[12] Lustini, F. G. Anwar, T. Lau, D. Chow, Victor, B. Yanto, A. Suwandi, and R. E. Saragih, "Carry and Go (CAGO): Robot AGV untuk penyortiran paket berbasis pemrosesan citra," Journal of Digital Ecosystem for Natural Sustainability, vol. 5, no. 1, pp. 1-10, 2025.

[13] S. Oktavia, Hendry, M. Naufal, R. Satyawira, N. Anuari, F. Cecillia, A. Suwandi, and R. E. Saragih, "Glambot SNAFH-R1: Lengan kamera 4-DOF biaya rendah untuk photobooth indoor berbasis pengolahan citra," Journal of Digital Ecosystem for Natural Sustainability, vol. 5, no. 2, pp. 76-85, 2025.

[14] M. T. Sepahi, H. Abusalma, V. Jovanovic, and H. Eisazadeh, "Mechanical properties of 3D-printed parts made of polyethylene terephthalate glycol," Journal of Materials Engineering and Performance, vol. 30, no. 9, pp. 6851-6861, 2021.

[15] M. A. R. Maulidin, T. N. Ali, and M. I. Mustofa, "Perancangan sistem monitoring penggunaan air PAM berbasis IoT dengan bot Telegram," Indonesian Journal of Technology, Informatics and Science, vol. 2, no. 1, pp. 46-50, 2020.

[16] R. T. H. Hasan and A. B. Sallow, "Face detection and recognition using OpenCV," Journal of Soft Computing and Data Mining, vol. 2, no. 2, pp. 86-97, 2021.

[17] S. O. Adeshina, H. Ibrahim, S. S. Teoh, and S. C. Hoo, "Custom face classification model for classroom using haar-like and LBP features with their performance comparisons," Electronics, vol. 10, no. 2, p. 102, 2021.

[18] C. Cruz Ulloa, G. Prieto Sanchez, A. Barrientos, and J. Del Cerro, "Autonomous thermal vision robotic system for victims recognition in search and rescue missions," Sensors, vol. 21, no. 21, p. 7346, 2021.

[19] J. Jaruenpunyasak, A. Garcia Seco de Herrera, and R. Duangsoithong, "Anthropometric ratios for lower-body detection based on deep learning and traditional methods," Applied Sciences, vol. 12, no. 5, p. 2678, 2022.

[20] K. C. V. G. Macaraeg, C. A. G. Hilario, and C. D. C. Ambatali, "LoRa-based mesh network for off-grid emergency communications," in Proc. IEEE Global Humanitarian Technology Conference (GHTC), Seattle, WA, USA, 2020, pp. 1-4.

[21] Undang-Undang Republik Indonesia Nomor 27 Tahun 2022 tentang Pelindungan Data Pribadi (Law of the Republic of Indonesia No. 27 of 2022 on Personal Data Protection), 2022.